BRAZILIAN JOURNAL OF FOOD TECHNOLOGY

ISSN 1981-6723
Online version

ORIGINAL ARTICLE

Physicochemical properties of extrudate-based flakes from whole banana flour and rice flour blends

Ronel Joel Bazán-Colque[1]*, Fiorella Ivette Ruiz-Barreto[1], Jhony Willian Vargas-Solórzano[1], Arturo Meléndez-Arévalo[1], José Luis Ramírez Ascheri[2]

[1]Universidade Federal Rural do Rio de Janeiro (UFRRJ), Programa de Pós-Graduação em Ciência e Tecnologia de Alimentos (PPGCTA), Seropédica/RJ - Brasil
[2]Embrapa Agroindústria de Alimentos, Guaratiba/RJ - Brasil

***Corresponding Author:** Ronel Joel Bazán-Colque, Universidade Federal Rural do Rio de Janeiro (UFRRJ), Programa de Pós-Graduação em Ciência e Tecnologia de Alimentos (PPGCTA), Rodovia BR 465, km 07, CEP: 23890-000, Seropédica/RJ - Brasil, e-mail: rjoelbazanc@ufrrj.br

Cite as: Bazán-Colque, R. J., Ruiz-Barreto, F. I., Vargas-Solórzano, J. W., Meléndez-Arévalo, A., & Ramirez Ascheri, J. L. (2023). Physicochemical properties of extrudate-based flakes from whole banana flour and rice flour blends. *Brazilian Journal of Food Technology*, *26*, e2023029. https://doi.org/10.1590/1981-6723.02923

Abstract

This study aimed to understand how adding whole-banana flour (*WBF*) affected the physicochemical properties of extrudates intended for the development of breakfast flakes. The parameters: *WBF* addition (50% to 70%, dry basis), feed moisture (27% to 33%, wet basis), and barrel temperature in the last zone of the extruder (80 ºC to 100 °C) were varied according to a 2^3 factorial design with augmented center points. The addition of *WBF* linearly affected all the physical and chemical properties evaluated and showed a synergistic effect with barrel temperature for changes in hardness and carbohydrate content. *WBF* additions above 64.9%, adjusted to feed moisture between 29.6% to 32.6%, and thermomechanically cooked at barrel temperatures above 87 °C, consumed 216 to 257 kJ/kg of mechanical energy, which produced flakes with a hardness between 160 and 180 N. This work could contribute to the incorporation of *WBF* for developing more nutritious breakfast cereals, with a fiber content greater than 7.2 g/100 g.

Keywords: Flour mix; Extrusion cooking; Physicochemical properties; Fiber-rich product; Optimization; Whole-banana.

Highlights

- Whole banana flour is a natural source of dietary fiber, vitamins, and minerals, which works well in the development of breakfast flakes
- Flakes made from whole banana and rice flour are naturally gluten-free, making them an excellent choice for those with celiac disease or gluten intolerance
- Whole banana flour positively affects the physicochemical properties of extruded flakes

1 Introduction

Green banana flour is a promising ingredient for developing novel products, either as pulp flour (Campuzano et al., 2018) or whole flour (Khoozani et al., 2020). While the search for alternative substitutes

to wheat flour continues as well as to provide sustainable by-product management, other forms of green banana flour consumption should be attempted. The peel contains healthy compounds, such as minerals and phenolic compounds (Pico et al., 2019), and increases lipids, proteins, and dietary fiber (Khoozani et al., 2019). This characteristic composition, together with the resistant starch provided by the pulp (Garcia-Valle et al., 2020), makes *WBF* a functional ingredient that stimulates intestinal peristalsis, fermentative capacity in the digestive tract, bowel evacuation, and a low glycemic index (Patiño-Rodríguez et al., 2019).

Breakfast flakes are conventionally produced by hydrothermal treatment or extrusion following the flaking of pellets, usually using cereal flours such as wheat, corn, and rice (Fast & Caldwell, 2000). Several breakfast cereal-like products have been formulated by partially replacing these cereal flours with other sources such as black gram (flaxseed) (Rani et al., 2020), cowpea bean (Marengo et al., 2017), and banana flour (Borah et al., 2016; Kaur et al., 2015). However, the inclusion of fiber-rich flour from non-conventional sources affects pellet texture and extrudate solubility; therefore, appropriate incorporation must be determined so that it does not significantly affect these properties. There is limited information in the literature on the use of *WBF* to formulate food products. Kaur et al. (2015) replaced 0 to 30% banana pulp flour in the development of a breakfast based on corn, and Borah et al. (2016) used 10% to 30% seeded banana flour during the formulation of breakfast cereal based on low-amylose rice flour and carambola pomace. Higher inclusions of could ensure more nutritive final products, with a prebiotic function, due to the fiber content effect in the gastrointestinal tract (Patiño-Rodríguez et al., 2019). Khoozani et al. (2020) developed bread by replacing wheat flour with *WBF* in the range of 10% to 30%, reaching 5.92% resistant starch in bread formulated with 30% of *WBF*.

Other important independent variables during extrudate production are feed moisture and barrel temperature profiles (Leonard et al., 2020; Masli et al., 2018). This moisture range was sufficient for pellet formation. For whole wheat flour, pellet moisture levels must be between 22% and 24%. The necessary heat input to the barrel must ensure dough cooking, considering that the zone temperature near the feeding point must be sufficiently low to prevent the start of starch conversion (Fast & Caldwell, 2000). Starch conversion monitoring during the extrusion process is carried out through specific mechanical energy (*SME*) input, whereas for extrudates (extruded flour suspensions), it is performed by measuring the water solubility index (*WSI*) and paste viscosity parameters. Accordingly, it was proposed to explore feeding blend moisture in the range of 27% to 33% and barrel temperatures in the last zone of 80 °C to 100 °C. These changes can affect the texture, solubility, and chemical composition of extrudates. The texture of breakfast flakes must be harder than that of extruded snacks because, as they are gradually hydrated during consumption with milk, they must retain the desired crunchy texture for a longer time. The final texture of flakes depends on the degree of pellet flattening, which is fitted by the roller rotation speed and roll gap, and its subsequent drying (Fast & Caldwell, 2000). The hardness (*HD*) of the bulk flake portion is the usual parameter for determining the instrumental texture of breakfast cereals (Leonard et al., 2020). Thus, this study aimed to evaluate the effects of *WBF* addition, feed moisture, and barrel temperature in the last zone of the extruder on starch conversion during the extrusion process (*SME*), starch conversion on flakes (*WSI* and paste viscosity parameters), *HD*, and proximal chemical composition of extruded ready-to-eat whole-banana breakfast flakes. In addition, the optimal region was determined using multiple desirable characteristics of the final product.

2 Materials and Methods

2.1 Materials

White rice grains were acquired from Fumacense Food Ltd. (Santa Catarina, Brazil). Banana fruits ("Terra" variety, genotype AAB) in the third stage of ripening were acquired from a central supply market (*CEASA*, Rio de Janeiro, Brazil) according to the maturation scale described by Gomes et al. (2013). The banana fruits were washed, immersed in chlorinated water (50 ppm/10 min), rinsed, and drained (3 min). The

fruits were then sliced approximately 5 mm thick, submerged in boiling water (3 min), slipped, placed on perforated trays, and dried for 20 h in a Hauber oven (DMS-G-EG, Santa Catarina, Brazil) at 60 °C.

2.2 Preparation of flours

White rice grains and dehydrated whole-banana slices were ground under the same conditions in a knife-hammer mill (TREU, 1188 model, São Paulo, Brazil), in which a 1.0 mm aperture screening plate was coupled. The milled products, *WBF* and *RF* were packed in low-density polyethylene (LDPE) bags and stored until further use.

2.3 Particle-size distribution

Particle-size distribution of the raw flours was determined by sieving analysis (American Society of Agricultural and Biological Engineers, 2008). The sample (100 g) was segregated through a set of six standard stainless-steel sieves (297, 212, 149, 106, 90, and 75 µm) and a pan (Newark, USA), using a ROTAP RX-29-10 (WS Tyler, St Albans, USA) for 10 min.

2.4 Preparation of feeding blends

The raw flours were blended in proportions according to the experimental design (Table 1). For each trial, blends of 500 g were manually prepared in LDPE bags. A water-appropriate amount (W, g) was added to adjust the moisture content according to Equation 1.

$$W = B \times \frac{(M_f - M_0)}{(100 - M_f)} \quad (1)$$

where B is the blend's mass to be moistened (500 g), M_0 is the blend's initial moisture, determined in duplicate by the oven method at 105 °C for 4 h (Association of Official Analytical Chemists, 2005), and M_f is the blend's final moisture (g/100 g, wet basis).

2.5 Extrusion process

The moistened blends were processed using a single-screw extruder 19/20 DN (Brabender, Duisburg, Germany) equipped with an internal grooved barrel, three electric heating zones, and an L/D ratio of 20. A standard screw attached to the barrel had a compression ratio of 3:1. A 3.0 mm diameter single cylindrical hole die was attached at the output of the third heating zone. The blends were fed using a single-screw volumetric feeder (Brabender, Duisburg, Germany). The feeding rate was set at ~ 4 kg/h. Extruder operational variables such as screw speed (120 rpm), barrel temperature profile (zone 1: 50 °C; zone 2: 70 °C; zone 3: according to the experimental design, Table 1), and torque values (N m) were monitored using WINEXT software, v 4.4.0 (Brabender, Duisburg, Germany). Once the process reached steady-state conditions for each trial, extrudates were collected. Mass flow at the beginning and end of each collection was measured in duplicate by collecting the amount of extrudate for 30 s.

2.6 Starch conversion during the extrusion process

Specific mechanical energy (*SME*) was calculated according to Equation 2.

$$SME = \frac{T \times (2\pi SS) \times n}{Q} \quad (2)$$

where T is the torque (N m) recorded at the time of collection, SS is screw speed which was kept constant at 120 rpm, n is the number of screws (n = 1), and Q is extrudate mass flow..

2.7 Preparation of flakes and extruded flours

In the intermediate stage of collection, the extrudate stream was coupled to a CL 300 roll laminator (G. Paniz, Rio Grande do Sul, Brazil), and laminated extrudates were cut into strips approximately 40 cm in length. The strips were then manually cut to produce square-shaped flakes of approximately 10.0 mm per side. Moist flakes were dried at 60 °C under the same conditions to produce dehydrated whole banana slices. The dried flakes were stored in polyethylene bags at room temperature for further analysis. The dried flake portion of each trial was ground in a disc mill LM3600 (Perten Instruments AB, Huddinge, Sweden) set to aperture 2. Then, the ground products were powdered in a hammer-mill LM3100 (Perten Instruments AB, Huddinge, Sweden) fitted with a 0.8 mm sieve aperture to reach a desirable particle size for analysis. The extruded flours were packed in LDPE bags and stored at room temperature for further analysis.

2.8 Hardness (*HD*)

The *HD* of the extruded flakes was determined by a compression test using a texture analyzer (TA.TXplus, Stable Micro Systems, UK), in which a 30 kg load cell and a 50 mm diameter compression plunger were coupled. Dry flakes were poured into a cylindrical container with a diameter of 52 mm and a height of approximately 30 mm (15 g sample). The compression accessory descended at a speed of 2 mm/s and deformed the flake bed to 30% of its initial height. After the test, the compression plunger ascended at 10 mm/s. For each trial, 15 repetitions were performed, and hardness was expressed as the maximum force (N) along the force-distance curve.

2.9 Starch conversion in the raw and extruded flours

Raw and extruded flours were sieved and particles between 106 and 212 μm were used for starch conversion analyses.

2.9.1 Water solubility index (*WSI*)

Suspension preparation and solubilization processes were performed according to the methodology described by Vargas-Solórzano et al. (2014).

2.9.2 Paste viscosity

The paste viscosity profiles were measured using a Rapid Viscosity Analyzer (*RVA*) series 4 (Newport Scientific Pty Ltd., Warriewood, Australia). The suspensions were prepared by adding 3 g of the sample (14% moisture) to 25 g of distilled water in an *RVA* aluminum cup. The paddle rotating speed was 160 rpm and the time-temperature profile started at 25 °C for 2 min, then heated to 95 °C, maintained at that temperature for 3 min, and then cooled to 25 °C, completing the test within 20 min. The heating and cooling stages were performed at 14 °C/min. The determined paste viscosity parameters were peak viscosity at 95 °C (*PV*) and setback viscosity (*SB*).

2.10 Proximal chemical composition

The proximal composition and dietary fiber content of raw and extruded flours were analyzed according to the official methods of the Association of Official Analytical Chemists (2005). The moisture and ash contents were determined using a TGA-2000 thermogravimetric analyzer (TGA) (Navas Instruments,

Conway, USA) at 105 °C and 550 °C, respectively, up to constant weight. Lipid content (*LIP*) was measured using the Soxhlet method 945.38, total nitrogen was measured using the Kjeldahl method 2001.11, protein content (*PRO*) was estimated as 5.75 × total nitrogen, and dietary fiber (*FIB*) was measured using the enzymatic-gravimetric method 985.29. The Carbohydrate content (*CHO*) was calculated from the difference.

2.11 Experimental design and statistical analysis

The experiment was arranged in a 2^3 factorial design with four augmented central points. The established levels were chosen based on preliminary trials and consulted the literature. The independent variables (X_1: whole-banana flour addition, X_2: feed moisture, and X_3: barrel temperature in the last zone) and responses (physical properties and proximal chemical composition) are presented in Table 1. A two-interaction linear model was tested according to Equation 3, to represent the behavior of each response in terms of the studied independent variables. The statistical significance of each term in the equation was determined by Analysis of Variance (*ANOVA*) at 5%, and 1% and regression analysis (Table 2).

$$\hat{Y} = \hat{\beta}_0 + \hat{\beta}_1 X_1 + \hat{\beta}_2 X_2 + \hat{\beta}_3 X_3 + \hat{\beta}_{12} X_1 X_2 + \hat{\beta}_{13} X_1 X_3 + \hat{\beta}_{23} X_2 X_3 \quad (3)$$

where $\hat{Y}$ is the estimated response, $\hat{\beta}_0$ is the intercept; $\hat{\beta}_1$, $\hat{\beta}_2$, and $\hat{\beta}_3$ represent the linear terms; $\hat{\beta}_{12}$, $\hat{\beta}_{13}$, and $\hat{\beta}_{23}$ represent the interaction terms; and X_1, X_2, and X_3 are independent variables. Response surface plots were generated for the adjusted models with no significant lack of fit (*LoF*) and a coefficient of determination (R^2) > 0.70.

The level curves selected for each response were superimposed to determine the optimal regions of operation from the technological and nutritional perspectives. Multiple response analysis was performed by reducing data variability to two principal components in which correlations among responses were evaluated. Statistical software (version 12.0; StatSoft, Tulsa, USA) was used to analyze the aforementioned statistical methods. Correlations below 0.5 were considered weak and above 0.8 were strong (Montgomery & Runger, 2018).

3 Results and Discussion

3.1 Particle-size distribution

Particle-size distributions were different for the *WBF* and *RF* ($p < 0.05$, Figure 1a). The *WBF* had 59% of particles ≤ 75 μm, whereas the *RF* had 31% of particles between 106 and 150 μm. The differences in particle size could be attributed to the composition of the food matrix between *WBF* and *RF* (Table 1). Endosperm hardness in rice grains is due to its starch granules embedded in a protein matrix (Chandrasekhar & Chattopadhyay, 1990), while the mesocarp in banana pulp is rich in soluble fibers (Khoozani et al., 2019), and its starch is poorly associated with protein. These structural tissues are broken in different ways during the grinding process, resulting in different shapes and particle-size distributions for both ingredients (Vargas-Solórzano et al., 2020). Particle size influences the water absorption rate. Particles smaller than 180 μm absorb more water during material wetting (Oladunmoye et al., 2014). The flours used in the experiment had 85.1% and 77.8% particles ≤ 150 μm for *WBF* and *RF*, respectively, which allowed uniform wetting before extrusion processing.

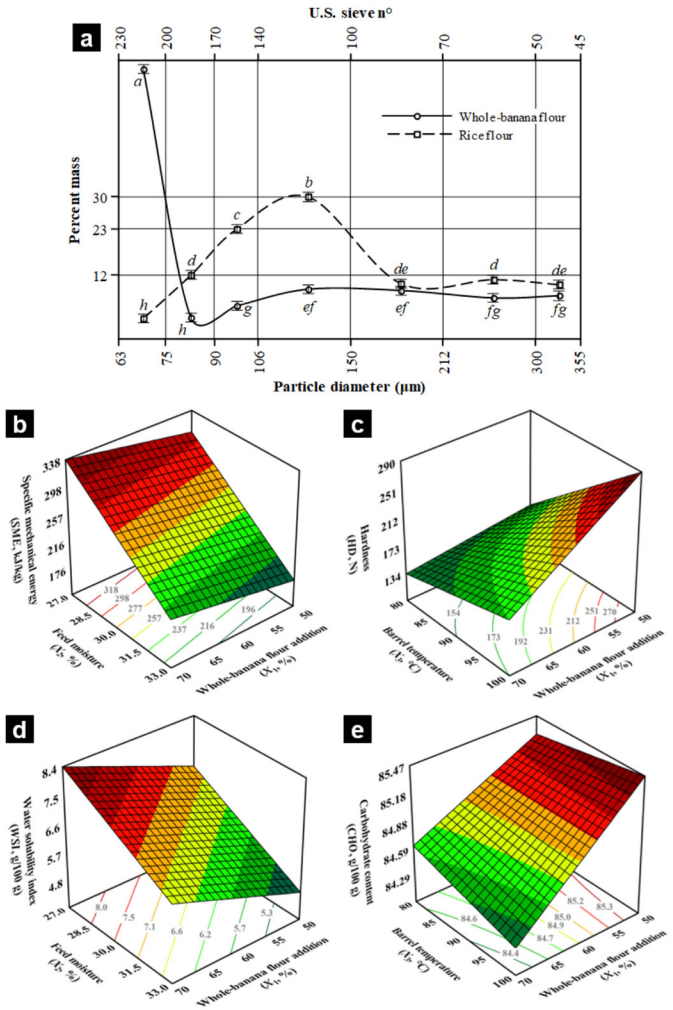

Figure 1. Particle-size distributions of whole-banana and rice flours (a). Response surface plots for (b) specific mechanical energy (SME, kJ/kg), (c) hardness (HD, N), (d) water solubility index (WSI, g/100 g), and (e) carbohydrate content (CHO, g/100 g).

Table 1. Experimental design and responses for physical properties and proximal chemical composition of extruded flakes and raw flours.

Trial	Experimental design			Physical property					Chemical composition [a] (g/100 g)				
	X_1	X_2	X_3	*SME*	*HD*	*WSI*[a]	*PV*	*SB*	*ASH*	*PRO*	*LIP*	*FIB*	*CHO*
	%	%	°C	kJ/kg	N	g [b]/100 g	mPa.s	mPa.s					
1	50	27	80	338.15	165.57	7.70	701.00	694.75	1.89	5.69	0.36	6.81	85.25
2	70	27	80	344.98	138.26	8.62	596.00	678.00	2.44	5.09	0.49	7.23	84.75
3	50	33	80	191.61	111.49	4.81	826.50	838.75	1.98	5.77	0.30	6.42	85.54
4	70	33	80	215.23	97.02	6.76	742.50	775.25	2.50	5.07	0.42	7.29	84.73
5	50	27	100	283.83	254.14	6.42	707.50	756.75	2.02	5.82	0.33	6.25	85.58
6	70	27	100	343.63	183.69	8.49	562.50	657.75	2.67	5.04	0.53	7.51	84.26
7	50	33	100	171.60	292.21	5.08	813.50	880.75	1.97	5.77	0.33	6.33	85.60
8	70	33	100	209.67	129.41	6.63	745.50	786.75	2.69	5.01	0.51	7.24	84.56
9	60	30	90	236.58	234.82	6.01	775.00	763.75	2.43	5.27	0.42	7.29	84.59
10	60	30	90	240.38	215.36	6.41	772.50	740.25	2.39	5.37	0.32	7.16	84.76
11	60	30	90	253.92	232.82	6.39	778.00	745.75	2.30	5.52	0.33	7.08	84.77
12	60	30	90	254.78	200.93	6.20	807.00	785.50	2.43	5.28	0.39	7.29	84.60
Raw materials													
Whole-banana flour (*WBF*)						7.47	2383.0	2583.25	4.30	3.96	1.10	10.58	80.05
Rice flour (*RF*)						1.15	2510.0	4983.75	1.68	7.54	0.87	1.08	88.82

X_1: WBF addition; X_2: feed moisture; X_3: barrel temperature in the last zone; *SME*: specific mechanical energy; *HD*: hardness; *WSI*: water solubility index; *PV*: peak viscosity; *SB*: setback viscosity; *ASH*: ash content; *PRO*: protein; *LIP*: lipid; *FIB*: dietary fiber; *CHO*: carbohydrates; [a]dry basis; [b]grams of soluble solids.

3.2 Effect of extrusion process on *SME*

SME values are presented in Table 1 and ranged from 171.6 to 345.0 kJ/kg. According to the *ANOVA* data (Table 2), the process variability was explained by the main effects of X_2 (87.92%, $p < 0.01$) and X_1 (5.30%, $p < 0.05$). The adjusted model had a non-significant *LoF* ($p > 0.05$) and good R^2 (0.932), which could be used for predictive purposes. The regression coefficients of the fitted models are presented in Table 2. The $\hat{\beta}_2$ had a high negative impact (–65.31) and the $\hat{\beta}_1$ had a low positive impact (+16.04), on *SME* values (Figure 1b). The *SME* increases either by reducing the moisture or increasing the fiber content in the feed material. This occurs because of a lower lubricating effect at low moisture levels (Mazlan et al., 2020), and insoluble fibers are hard to melt, hindering the flow of molten material and consequently increasing the torque. The *SME* is also affected by the particle size that structures a feed material. Fine particles are compacted to a greater extent and can increase the torque (Carvalho et al., 2010). In this study, the feed material was composed of particles smaller than 355 μm, which could have also contributed to the increasing *SME* values. However, the X_3 did not affect the *SME* in the studied interval. During extrusion cooking experiments, temperature changes of approximately 20 °C were not significant for the *SME* values (Altan et al., 2008; Bastos-Cardoso et al., 2007). Low-temperature profiles in the barrel are desirable for economizing energy and processing costs.

Table 2. Sum of squares (*SS*) of the adjusted *ANOVA* and regression coefficients (in coded levels) of the adjusted models for physical properties and chemical composition of extruded flakes.

	Physical properties					Proximal chemical composition				
	SME	***HD***	***WSI***	***PV***	***SB***	***ASH***	***PRO***	***LIP***	***FIB***	***CHO***
Effect										
X_1	2058.3*	9455.2**	5.27**	20200.5**	9333.2*	0.74**	1.01**	0.05*	1.50**	1.68**
X_2	34123.2**	--	7.90**	39340.1**	30535.4**	--	--	--	--	--
X_3	--	15060.7**	--	--	--	--	--	--	--	0.01^{ns}
X_{12}	--	--	--	--	--	--	--	--	--	--
X_{13}	--	4582.6*	--	--	--	--	--	--	--	0.14*
X_{23}	--	--	--	--	--	--	--	--	--	--
L_0F	2371.0^{ns}	11046.8^{ns}	1.75^{ns}	15409.3*	3293.2^{ns}	0.09^{ns}	0.02^{ns}	0.01^{ns}	0.51^{ns}	0.42^{ns}
PE	259.4	765.3	0.11	775.2	1251.8	0.01	0.04	0.01	0.03	0.03
SS_{total}	38811.9	40910.6	15.02	75725.1	44413.5	0.85	1.07	0.07	2.04	2.28
R^2	0.93	0.71	0.88	0.79	0.90	0.88	0.95	0.71	0.73	0.80
Coeff.										
$\hat{\beta}_0$	257.03**	187.98**	6.63**	735.63**	758.67**	2.31**	5.39**	0.39**	6.99**	84.92**
$\hat{\beta}_1$	16.04*	-34.38**	0.81**	-50.25**	-34.16*	0.31**	-0.36**	0.08*	0.43**	-0.46**
$\hat{\beta}_2$	-65.31**	--	-0.99**	70.13**	61.78**	--	--	--	--	--
$\hat{\beta}_3$	--	43.39**	--	--	--	--	--	--	--	-0.03^{ns}
$\hat{\beta}_{12}$	--	--	--	--	--	--	--	--	--	--
$\hat{\beta}_{13}$	--	-23.93*	--	--	--	--	--	--	--	-0.13*
$\hat{\beta}_{23}$	--	--	--	--	--	--	--	--	--	--

X_i: main effects; X_{ij}: interaction effects; subscripts 1: *WBF* addition, 2: feed moisture, and 3: barrel temperature in the last zone; *LoF*: lack of fit; *PE*: pure error; *SS*: sum of squares. *SME*: specific mechanical energy; *HD*: hardness; *WSI*: water solubility index; *PV*: peak viscosity; *SB*: setback viscosity; *ASH*: ash content; *PRO*: protein content; *LIP*: lipid content; *FIB*: dietary fiber; *CHO*: carbohydrate content. *Significant at $p < 0.05$; **Significant at $p < 0.01$; ^{ns}not significant.

3.3 Effect of extrusion process on *HD*

Flake hardness (*HD*) was measured as the maximum force required to compress a cylindrical bed of flakes of a fixed height. The flakes produced from the extrudates were flattened by rollers in which the air cell structures were broken, yielding *HD* values between 97.02 and 292.21 N (Table 1). These values are higher than the *HD* of commercial corn flakes (64.8 ± 6.28 N) determined using the same method. Based on the ANOVA data (Table 2), process variability was explained by all effects in the following order: X_3 (36.81%,

$p < 0.01$), X_1 (23.11%, $p < 0.01$), and the interaction effect X_{13} (10.41%, $p < 0.05$). The linear model with the interaction test showed a non-significant *LoF* ($p > 0.05$) and acceptable R^2 (0.711), which could be used to predict future values within the studied range. Changes in X_3 from 80 to 100 °C slightly increased *HD*, whereas changes in X_1 from 50 to 70% considerably decreased *HD* (Figure 1c). Furthermore, the interaction effect X_1X_3 also decreased *HD*. The regression coefficients of the fitted models are presented in Table 2. The $\hat{\beta}_3$ had a high positive value (+43.39) and contributed to increasing *HD*, whereas $\hat{\beta}_1$ and $\hat{\beta}_{13}$ showed negative values (–4.38 and –23.93, respectively) and contributed to decreasing *HD*. Extruded products based on banana/maize showed *HD* values from 30.2 to 56.6 N (Oduro-Yeboah et al., 2014), and 51.35 to 138.39 N (Kaur et al., 2015). These low values can be attributed to the air cell structures preserved in the extruded products, unlike those in the flattened products obtained in this study. This could be attributed to the soluble fiber content present in the banana pulp, which represents 60% of the fruit's overall weight, as well as to the pectin and gums of the banana peel (Khoozani et al., 2019). It appears that the hardness of the flakes has an inverse relationship with the content of soluble fibers in the feed material. The flakes obtained from extrudates with 70% addition of whole-banana flour presented a lower *HD*.

3.4 Effect of extrusion process on *WSI*

The *WSI* values represent the soluble polysaccharide content released in excess water and are related to the starch conversion of extruded products (Kaur et al., 2015). When comparing the *WSI* of both raw materials, *WBF* was approximately 6.5-fold higher than that of *RF* ($p < 0.05$, Table 1). These differences may be related to the composition of sugars and soluble fibers in the bulkier fraction of both raw materials: the mesocarp in bananas and the endosperm in rice. The extrusion increased the *WSI* values from 4.81 to 8.62 g of soluble solids/100 g, which represented an increase from 11.86 to 79.07% when compared to raw blends (7.47 and 1.15 g soluble solids/100 g for *WBF* and *RF*, respectively, Table 1). According to the ANOVA data (Table 2), process variability was explained by the main effects of X_2 (52.6%, $p < 0.01$) and X_1 (35.09%, $p < 0.01$) (Table 2). The linear model used in the experiment showed an acceptable R^2 (0.877) and non-significant *LoF* ($p > 0.05$). Changes in X_1 from 50% to 70% slightly increased *WSI*. A similar behavior was observed during the production of extrudates based on corn and banana (Kaur et al., 2015). In contrast, changes in X_2 from 27% to 33% considerably decreased the WSI (Figure 1d). As confirmed by other studies, feed moisture has an inverse effect on the *WSI* of extruded products (Hagenimana et al., 2006; Sarawong et al., 2014). By increasing the moisture content of the feed material in the barrel temperature range of 80-100 °C, the starch conversion was reduced. This is because the greater lubricating effect of water prevents the breaking of starch granules and limits their gelatinization (Leonard et al., 2020). The $\hat{\beta}_2$ had a high negative value (–0.99) and contributed to decreasing *WSI*, whereas $\hat{\beta}_1$ showed a positive value (+0.81) and contributed to increasing *WSI* (Table 2).

3.5 Effect of extrusion process on paste viscosity

The paste viscosity curve reveals the degree of gelatinization and molecular degradation of the starch granules (Carvalho et al., 2010). *PV* is the maximum on the viscosity curve in the heating range of 95 °C and establishes the limit between swelling and breakdown of the starch granules (Figure 2a). The peak time of *WBF* (8.4 min) was slightly shorter than that of *RF* (9.9 min). The *PV* values for the extruded products ranged from 562.5 to 826.5 mPa s, which decreased by 66.2% to 77.0% with respect to the raw flours (Table 1). Extruded products based on grain and banana flours showed *PV* values in the range of 298.50 to 703.00 mPa.s These differences can be attributed to the extrusion conditions. At higher feed moisture levels, fewer starch granules were converted; hence, the *PV* of these extruded flours was higher. In addition, as more *WBF* was added, the insoluble fiber content hindered the swelling of starch granules, and the *PV* of these extruded flours was lower (Figure 2a, b). On the other hand, the *SB* represents the increase in the viscosity curve during the cooling period. Differences in the *SB* of the raw materials showed that *RF* was approximately 2-fold higher than that of *WBF* ($p < 0.05$). According to the

domain explored to produce flakes, *SB* values ranged from 657.75 to 880.75 mPa s, which decreased by 76.7% to 82.6% with respect to the raw flours (Table 1). Extruded products based on grain and banana flours showed *SB* in the range of 437.5 to 1,421.5 mPa s (Oduro-Yeboah et al., 2014). These differences can be attributed to the degree of amylose lixiviation. The starch granules that are less converted in the extruded flour have the capacity to leach amylose, which retrogrades and raises the setback viscosity. In contrast, the insoluble fiber content in the extruded flour hindered amylose retrogradation and decreased the setback viscosity (Figure 2a, c). From the *ANOVA* data (Table 2), the main effects of X_2 (*PV*: 51.95%, *SB*: 68.75%) and X_1 (*PV*: 26.67%, *SB*: 21.01%) were significant ($p < 0.01$). The linear model used in the experiment showed acceptable R^2 (0.786 and 0.898 for *PV* and *SB*, respectively), a significant *LoF* for *PV* ($p < 0.05$), and a non-significant *LoF* for *SB* ($p > 0.05$). Changes in X_2 from 27 to 33% considerably increased *PV* and *SB*, whereas changes in X_1 from 50 to 70% slightly decreased *PV* and *SB* (Figure 2b, c). The $\hat{\beta}_2$ had high positive values (+70.13 and +61.78 for *PV* and *SB*, respectively) and contributed to increasing both responses, whereas the $\hat{\beta}_1$ showed low negative values (–50.25 and –34.16 for *PV* and *SB*, respectively) and contributed to decreasing both responses (Table 2). Figure 2b shows the degree of extrusion cooking according to the studied variables. Figure 2c shows the reorganization tendency of the starch polymers present in the banana-rice-based suspensions that were cooled. Extrudates produced at low levels of *WBF* and high levels of feed moisture maintained a greater amount of non-gelatinized or partly gelatinized starch granules, characteristic of less cooked products, associated with high *PV* (Sarawong et al., 2014), and high values of *SB* (Hagenimana et al., 2006).

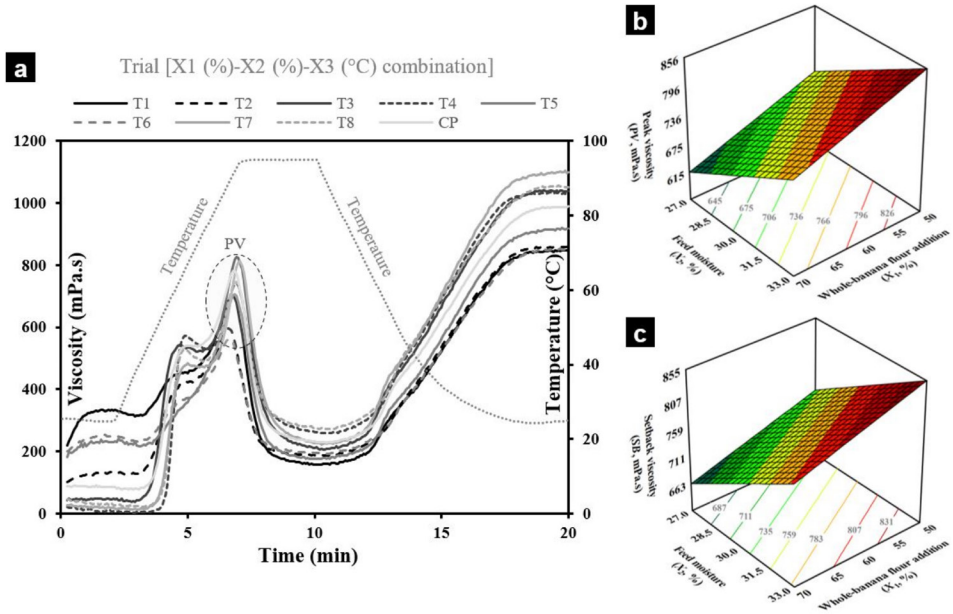

Figure 2. Paste viscosity profiles (a) and response surface plots for (b) peak viscosity (PV, mPa·s) and (c) setback viscosity (SB, mPa·s). CP: center-point treatment.

3.6. Effect of extrusion process on proximal chemical composition

The proximal chemical composition of the raw materials showed that *WBF* had approximately 10-fold more *FIB*, 2.5-fold more *ASH*, and half *PRO*, compared to *RF* (Table 1, $p < 0.05$). This difference could be attributed to the presence of more minerals complexed with fibers in the *WBF* (Kiewlicz & Rybicka, 2020). These complexes were more noticeable in the fruit peel and cereal pericarps. After extrusion, the proximal chemical composition of the extrudates was affected only by X_1. Compared to the starting blends, *ASH* and *LIP* contents decreased, whereas the varied inversely to X_1 levels, and the *PRO* remained unchanged (Figure 3). Gamlath (2008) also observed decreases in *ASH* and *LIP* contents during extrudate production based on blends of *RF* and banana flour at different ripening stages. *ASH* content of extrudates ranged from 1.89 to 2.69 g/100 g, and

FIB content from 6.25 to 7.51 g/100 g (Table 1). Gamlath (2008) reported *ASH* values for extrudates within the range found in this study; however, the *FIB* values were lower and varied according to the banana ripening stage in the mixture. The changes in *FIB* as a result of extrusion cooking are not well understood (Leonard et al., 2020).

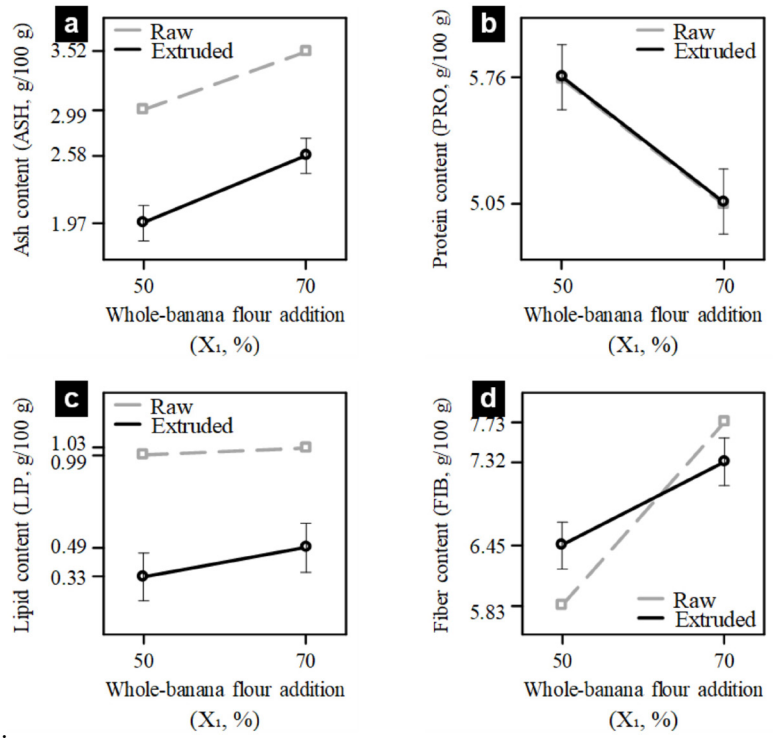

Figure 3. WBF addition effect plots for proximal composition (g/100 g): (a) ash content (ASH), (b) protein content (PRO), (c) lipid content (LIP), and (d) dietary fiber (FIB).

The changes observed in this study (Figure 3d) can be attributed to the excess fiber content in the feeding blend (X_1: 70%), which contributed to the formation of low-molecular-weight soluble fibers, as confirmed by the high *WSI* values (Figure 1d), which could not be recovered by alcohol precipitation during dietary fiber analysis. All extrudates obtained more than 5 g/100 g of dietary fiber and could be considered fiber-rich food sources (Li & Komarek, 2017). These fibers would include pectin, cellulose, lignin, and hemicellulose (Khoozani et al., 2019). Increasingly, consumers are looking for alternative gluten-free products rich in fiber to benefit their health. Fiber intake reduces the risk of cardiovascular disease, intestinal disorders, and colorectal cancer (Leonard et al., 2020). *ANOVA* (Table 2) confirmed that X_1 was the only factor that affected the proximal chemical composition of the extrudates (Figure 3), except for *CHO*, where the interaction term X_{13} was also influenced (Table 2, Figure 1e). The process variability due to X_1 was 87.06% for *ASH*, 94.39% for *PRO*, 73.53% for *FIB*, and 73.68% for *CHO* ($p < 0.01$), whereas that for *LIP* was 71.43% ($p < 0.05$). The linear model of *CHO* showed an acceptable R^2 (0.803), and non-significant *LoF* ($p > 0.05$), in which the negative values of $\hat{\beta}_1$ (–0.46) and $\hat{\beta}_{13}$ (–0.13) contributed to decreasing *CHO* content (Table 2). Furthermore, the *CHO* content was slightly affected by barrel temperature. By changing the temperature from 80 °C to 100 °C, the *CHO* increased or decreased, depending on whether the feed material had lower or higher *WBF* content, respectively.

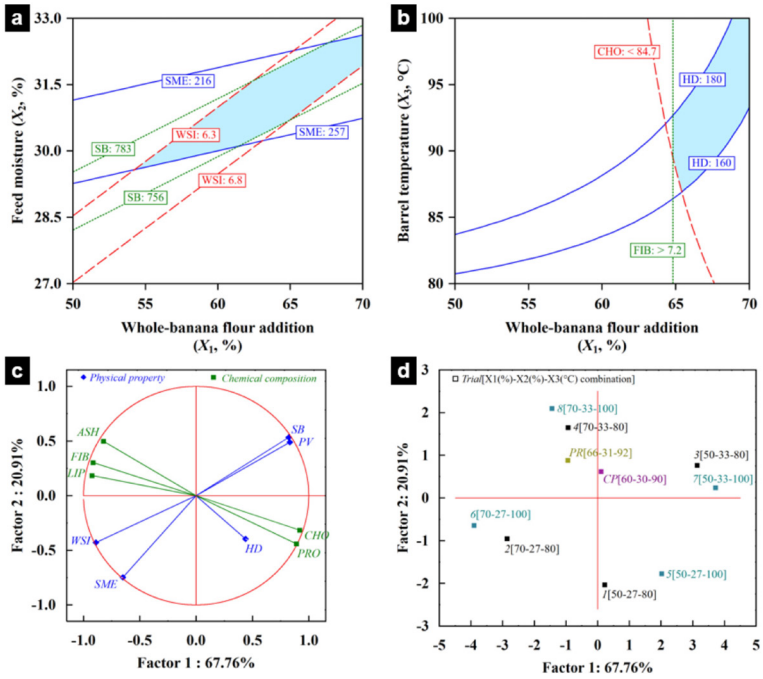

Figure 4. Region of the optimum found by overlaying response surfaces: (A) specific mechanical energy (SME, kJ/kg), water solubility index (WSI, g/100 g), and setback viscosity (SB, mPa s); (B) hardness (HD, N), carbohydrate content (CHO, g/100 g), and dietary fiber (FIB, g/100 g). Principal component analysis (PCA): (C) physical and chemical response correlation plot; (D) projection of the treatments on the factor map. CP: center-point treatment; PR: a predicted point within the optimal region.

3.7 Optimization process and principal component analysis (*PCA*)

Optimal extrusion conditions were obtained by superimposing contour graphs of *SME*, *WSI*, and *SB* over the X_1X_2 plane (Figure 4a), as well as *HD*, *CHO*, and *FIB* over the X_1X_3 plane (Figure 4b) to satisfy the technological and nutritional properties of the extruded flakes. Desirability ranges were as follows: $6.3 \leq WSI$ (g/100 g, dry basis) ≤ 6.8, $756 \leq SB$ (mPa s) ≤ 783, $7.2 \leq FIB$ (g/100 g, dry basis), and *CHO* (g/100 g, dry basis) ≤ 84.7. Figure 4a shows the feasible operating region from a technological standpoint, in the range of: $54.2{:}45.8 \leq X_1$ (%:%) $\leq 70{:}30$ and $29.6 \leq X_2$ (%) ≤ 32.6. On the other hand, Figure 4b shows the feasible operating region from the nutritional standpoint, in the range of $64.9{:}35.1 \leq X_1$ (%:%) $\leq 70{:}30$, and $87.0 \leq X_3$ (°C) ≤ 100. Under these conditions, the *SME* ranged between 216 and 257 kJ/kg which supplied the necessary energy for intermediate cooking of worked mixtures and produced flakes with *HD* between 160-180 N, necessary values to maintain product integrity gradually, when the flakes are soaked with milk during consumption. The flakes obtained in these regions guarantee both technological and nutritional characteristics, which are necessary for the development of novel products.

The dimensionality reduction of all responses as a set into two principal components allowed for the retention of more than 70% of the variation present in the original responses (88.67%). According to the response correlation plot (Figure 4c), the responses that presented strong positive correlations ($p < 0.01$) were: *PV-SB* (+0.85), *SME-WSI* (+0.89), *PRO-CHO* (+0.91), and *FIB-ASH* (+0.88). Correlations between *LIP-FIB* and *LIP-ASH* scores were intermediate ($p < 0.01$). Diagonally opposite responses presented strong negative correlations ($p < 0.01$), such as *SME-PV* (–0.85), *SME-SB* (–0.93), *WSI* with *PV* or *SB* (–0.93), *FIB-CHO* (–0.98), *ASH-PRO* (–0.95), *ASH-CHO* (–0.93), and *PRO-FIB* (–0.91). The smallest and largest angles formed between the two vectors belonging to different response groups (physical or chemical), were observed for *LIP-WSI* (the smallest) and *LIP-PV* (the largest), which is interpreted as moderate correlations between them (+0.69 and –0.70, respectively, $p < 0.05$). *HD* was the only response poorly represented by the principal components and did not correlate with any physical or chemical response. The projection of the treatments on the factor map (Figure 4d) confirms the small contribution

of X_3 to the data variability; that is, the change in barrel temperature from 80 to 100 °C was not significant in most of the assessed responses because factorial points 1 to 4 are close to factorial points 5 to 8. By analyzing Figure 4c and d together, it can also be confirmed which treatments presented maxima in the response surfaces for the physical properties shown in Figure 1, 2. In this way, trials 3 and 7 showed the highest *SB* and *PV* values, trials 2 and 6 the highest *WSI* and *SME* values, and trial 5 the highest *HD* value. However, given that chemical composition responses were only affected by X_1, trials 4 and 8 showed the highest *ASH*, *LIP*, and *FIB* values (X_1 = 70%), whereas trial 5 had the highest *PRO* value (X_1 = 50%). A specific point within the optimal region shown in Figure 4 a, b (X_1-X_2-X_3: 66% - 31% - 92 °C) was also projected as a predicted treatment (*PR*). As shown in Figure 4d, the *PR* point was positioned near the center-point treatment (*CP*) in trials 4 and 8. Intermediate values of *SME*, *WSI*, and *HD*, and high values of dietary fiber were achieved at this location.

4 Conclusion

The addition of whole banana flour (*WBF*) significantly modified the technological and nutritional properties of extruded flakes based on whole-banana/rice flour blends. By increasing the *WBF* in the feed blend, all physicochemical properties linearly increased. *WBF* addition showed a synergistic effect only with barrel temperature on changes in hardness and carbohydrate content. Meanwhile, feed moisture linearly affected the physical properties, except for hardness, and did not interact with other factors. In addition, an optimal region was identified using mathematical models developed from the responses. The results suggest that the *WBF* should be incorporated above 64.9% (dry basis), the raw blend moisture fixed between 29.6 and 32.6%, and the barrel temperature in the last zone maintained above 87 °C to produce extruded flakes with acceptable technological and nutritional characteristics: low *WSI* range (6.3 to 6.8 g/100 g), intermediate *HD* range (160 to 180 N) and a fiber content greater than 7.2 g/100 g. Overall, this work could contribute to the development of more nutritious breakfast cereals and diversify the range of existing gluten-free and high-fiber products on the market for people with gluten allergies and celiac disease. On the other hand, sustainable processing is proposed to obtain and use banana flour because the peel is used, and no waste is generated.

Acknowledgements

The authors thank to CAPES - Finance code 001, CNPq, and FAPERJ for their generous support to this work.

References

Altan, A., McCarthy, K. L., & Maskan, M. (2008). Extrusion cooking of barley flour and process parameter optimization by using response surface methodology. *Journal of the Science of Food and Agriculture*, *88*(9), 1648-1659. http://dx.doi.org/10.1002/jsfa.3262

American Society of Agricultural and Biological Engineers – ASABE. (2008). *Method of determining and expressing fineness of feed materials by sieving*. Michigan: ASABE.

Association of Official Analytical Chemists – AOAC. (2005). *Official methods of analysis* (18th ed.). Gaithersburg: AOAC International.

Bastos-Cardoso, I., Zazueta-Morales, J. D. J., Martínez-Bustos, F., & Kil-Chang, Y. (2007). Development and characterization of extruded pellets of whole potato (*Solanum tuberosum* L.) flour expanded by microwave heating. *Cereal Chemistry*, *84*(2), 137-144. http://dx.doi.org/10.1094/CCHEM-84-2-0137

Borah, A., Lata Mahanta, C., & Kalita, D. (2016). Optimization of process parameters for extrusion cooking of low amylose rice flour blended with seeded banana and carambola pomace for development of minerals and fiber rich breakfast cereal. *Journal of Food Science and Technology*, *53*(1), 221-232. PMid:26787944. http://dx.doi.org/10.1007/s13197-015-1772-9

Campuzano, A., Rosell, C. M., & Cornejo, F. (2018). Physicochemical and nutritional characteristics of banana flour during ripening. *Food Chemistry*, *256*, 11-17. PMid:29606425. http://dx.doi.org/10.1016/j.foodchem.2018.02.113

Carvalho, C. W. P., Takeiti, C. Y., Onwulata, C. I., & Pordesimo, L. O. (2010). Relative effect of particle size on the physical properties of corn meal extrudates: Effect of particle size on the extrusion of corn meal. *Journal of Food Engineering*, *98*(1), 103-109. http://dx.doi.org/10.1016/j.jfoodeng.2009.12.015

Chandrasekhar, P. R., & Chattopadhyay, P. K. (1990). Studies on microstructural changes of parboiled and puffed rice. *Journal of Food Processing and Preservation*, *14*(1), 27-37. http://dx.doi.org/10.1111/j.1745-4549.1990.tb00123.x

Fast, R. B., & Caldwell, E. F. (2000). *Breakfast cereals and how they are made* (2nd ed.). Minnesota: American Association of Cereal Chemists.. http://dx.doi.org/10.1094/1891127152.

Gamlath, S. (2008). Impact of ripening stages of banana flour on the quality of extruded products. *International Journal of Food Science & Technology*, *43*(9), 1541-1548. http://dx.doi.org/10.1111/j.1365-2621.2007.01574.x

Garcia-Valle, D. E., Agama-Acevedo, E., Alvarez-Ramirez, J., & Bello-Perez, L. A. (2020). Semolina pasta replaced with whole unripe plantain flour: Chemical, cooking quality, texture, and starch digestibility. *Stärke*, *72*(9-10), 1900097. http://dx.doi.org/10.1002/star.201900097

Gomes, J. F. S., Vieira, R. R., & Leta, F. R. (2013). Colorimetric indicator for classification of bananas during ripening. *Scientia Horticulturae*, *150*, 201-205. http://dx.doi.org/10.1016/j.scienta.2012.11.014

Hagenimana, A., Ding, X., & Fang, T. (2006). Evaluation of rice flour modified by extrusion cooking. *Journal of Cereal Science*, *43*(1), 38-46. http://dx.doi.org/10.1016/j.jcs.2005.09.003

Kaur, A., Kaur, S., Singh, M., Singh, N., Shevkani, K., & Singh, B. (2015). Effect of banana flour, screw speed and temperature on extrusion behaviour of corn extrudates. *Journal of Food Science and Technology*, *52*(7), 4276-4285. PMid:26139892. http://dx.doi.org/10.1007/s13197-014-1524-2

Khoozani, A. A., Birch, J., & Bekhit, A. E. D. A. (2019). Production, application and health effects of banana pulp and peel flour in the food industry. *Journal of Food Science and Technology*, *56*(2), 548-559. PMid:30906012. http://dx.doi.org/10.1007/s13197-018-03562-z

Khoozani, A. A., Kebede, B., Birch, J., & El-Din Ahmed Bekhit, A. (2020). The effect of bread fortification with whole green banana flour on its physicochemical, nutritional and in vitro digestibility. *Foods*, *9*(2), 152. PMid:32033343. http://dx.doi.org/10.3390/foods9020152

Kiewlicz, J., & Rybicka, I. (2020). Minerals and their bioavailability in relation to dietary fiber, phytates and tannins from gluten and gluten-free flakes. *Food Chemistry*, *305*, 125452. PMid:31514050. http://dx.doi.org/10.1016/j.foodchem.2019.125452

Leonard, W., Zhang, P., Ying, D., & Fang, Z. (2020). Application of extrusion technology in plant food processing byproducts: An overview. *Comprehensive Reviews in Food Science and Food Safety*, *19*(1), 218-246. PMid:33319515. http://dx.doi.org/10.1111/1541-4337.12514

Li, Y. O., & Komarek, A. R. (2017). Dietary fibre basics: Health, nutrition, analysis, and applications. *Food Quality and Safety*, *1*(1), 47-59. http://dx.doi.org/10.1093/fqs/fyx007

Marengo, M., Baffour, L. C., Buratti, S., Benedetti, S., Saalia, F. K., Carpen, A., Manful, J., Johnson, P. N. T., Barbiroli, A., Bonomi, F., Pagani, A., Marti, A., & Iametti, S. (2017). Defining the overall quality of cowpea-enriched rice-based breakfast cereals. *Cereal Chemistry*, *94*(1), 151-157. http://dx.doi.org/10.1094/CCHEM-04-16-0092-FI

Masli, M. D. P., Gu, B. J., Rasco, B. A., & Ganjyal, G. M. (2018). Fiber-rich food processing byproducts enhance the expansion of cornstarch extrudates. *Journal of Food Science*, *83*(10), 2500-2510. PMid:30211951. http://dx.doi.org/10.1111/1750-3841.14290

Mazlan, M. M., Talib, R. A., Taip, F. S., Chin, N. L., Sulaiman, R., Shukri, R., & Mohd Nor, M. Z. (2020). Changes in the physical properties and specific mechanical energy of corn-mango peel extrudates. *CYTA: Journal of Food*, *18*(1), 417-426. http://dx.doi.org/10.1080/19476337.2020.1767693

Montgomery, D. C., & Runger, G. C. (2018). *Applied statistics and probability for engineers* (7th ed.). Hoboken: John Wiley & Sons.

Oduro-Yeboah, C., Onwulata, C., Tortoe, C., & Thomas-Gahring, A. (2014). Functional Properties of Plantain, Cowpea Flours and Oat Fiber in Extruded Products. *Journal of Food Processing and Preservation*, *38*(1), 347-355. http://dx.doi.org/10.1111/j.1745-4549.2012.00782.x

Oladunmoye, O. O., Aworh, O. C., Maziya-Dixon, B., Erukainure, O. L., & Elemo, G. N. (2014). Chemical and functional properties of cassava starch, durum wheat semolina flour, and their blends. *Food Science & Nutrition*, *2*(2), 132-138. PMid:24804071. http://dx.doi.org/10.1002/fsn3.83

Patiño-Rodríguez, O., Agama-Acevedo, E., Pacheco-Vargas, G., Alvarez-Ramirez, J., & Bello-Pérez, L. A. (2019). Physicochemical, microstructural and digestibility analysis of gluten-free spaghetti of whole unripe plantain flour. *Food Chemistry*, *298*, 125085. PMid:31260951. http://dx.doi.org/10.1016/j.foodchem.2019.125085

Pico, J., Xu, K., Guo, M., Mohamedshah, Z., Ferruzzi, M. G., & Martinez, M. M. (2019). Manufacturing the ultimate green banana flour: Impact of drying and extrusion on phenolic profile and starch bioaccessibility. *Food Chemistry*, *297*, 124990. PMid:31253323. http://dx.doi.org/10.1016/j.foodchem.2019.124990

Rani, P., Kumar, A., Purohit, S. R., & Rao, P. S. (2020). Development of multigrain extruded flakes and their sensory analysis using fuzzy logic. *Journal of Food Measurement and Characterization*, *14*(1), 411-424. http://dx.doi.org/10.1007/s11694-019-00303-4

Sarawong, C., Schoenlechner, R., Sekiguchi, K., Berghofer, E., & Ng, P. K. W. (2014). Effect of extrusion cooking on the physicochemical properties, resistant starch, phenolic content and antioxidant capacities of green banana flour. *Food Chemistry*, *143*, 33-39. PMid:24054209. http://dx.doi.org/10.1016/j.foodchem.2013.07.081

Vargas-Solórzano, J. W., Ascheri, J. L. R., Carvalho, C. W. P., Takeiti, C. Y., & Galdeano, M. C. (2020). Impact of the pretreatment of grains on the interparticle porosity of feed material and the torque supplied during the extrusion of brown rice. *Food and Bioprocess Technology*, *13*(1), 88-100. http://dx.doi.org/10.1007/s11947-019-02379-8

Vargas-Solórzano, J. W., Carvalho, C. W. P., Takeiti, C. Y., Ascheri, J. L. R., & Queiroz, V. A. V. (2014). Physicochemical properties of expanded extrudates from colored sorghum genotypes. *Food Research International*, *55*, 37-44. http://dx.doi.org/10.1016/j.foodres.2013.10.023

Funding: Coordenação de Aperfeiçoamento de Pessoal de Nível Superior - CAPES (Finance code 001).

Received: Mar. 24, 2023; **Accepted:** Aug. 03, 2023

Associate Editor: Rosinelson da Silva Pena.